Mechanics of Composite Materials, Vol. 46, No. 4, 2010

SOLUTION OF A COUPLED PROBLEM OF THERMOPIEZOELECTRICITY BASED ON A GEOMETRICALLY EXACT SHELL ELEMENT

G. M. Kulikov* and V. Plotnikova

Keywords: *laminated piezoelectric shell, thermopiezoelectricity, 7-parameter shell model, geometrically exact shell element*

Based on a 7-parameter shell model, a numerical algorithm has been developed for solving a coupled problem of thermoelectroelasticity for a laminated piezoelectric shell subjected to a thermoelectromechanical loading. As unknowns, six tangential and transverse displacements of outer surfaces and the transverse displacement of shell midsurface are chosen. This choice provides a possibility of utilizing the complete 3D constitutive equations of thermopiezoelectricity. A geometrically exact 3D hybrid piezoelectric shell element is formulated by using nonconventional analytical integration. With the help of this finite element, solutions of coupled problems of thermoelectroelasticity for laminated plates and shells with segmented and distributed piezoelectric sensors and actuators are obtained.

Introduction

Under service conditions, thin-walled composite structures can undergo critical deformations and stresses caused by changes in the ambient temperature. In modern technologies, to counterbalance such deformations and to control the form of the structures, piezoelectric materials, placed in their body or fixed on their surface, are used. In this connection, new software products based on *isoparametric* three-dimensional finite shell elements with distributed piezoelectric sensors and actuators are actively being developed and introduced into industry [1-6]. A particular feature of such products is the fact that the initial and deformed configurations of a shell are interpolated uniformly in a global Cartesian system of coordinates, which makes it possible to correctly describe the rigid-body displacements of the shell. However, the isoparametric shell element is inefficient in calculating the adaptive composite structures, for which a fast response to undesirable external thermal and force actions is of great importance.

As an alternative, *geometrically* exact finite shell elements based on deformation relations of 6-, 7-, and 9-parameter 3-D shell models [7-10] may be used; they precisely represent the displacements of a shell as a rigid body in curvilinear coordinates of a reference surface. The term "geometrically exact" means that the reference surface of the shell is described by functions specified analytically, in particular, by splines, which serve as a basis for modern CAD systems. In this case, the vectors of

---

Tambov State Technical University, Russia. Translated from Mekhanika Kompozitnykh Materialov, Vol. 46, No. 4, pp. 513-534, July-August, 2010. Original article submitted May 19, 2009.

*Corresponding author; e-mail: kulikov@apmath.tstu.ru

0191-5665/10/4604-0349

displacements of external and median surfaces are represented in a local basis connected with the reference surface of the shell. Precisely this factor makes it possible to raise the capacity of a finite-element code and to use it efficiently in controllers of adaptive thin-walled structures.

In the present study, a new geometrically exact 7-parameter bilinear shell element is developed for calculating thin-walled composite structures with distributed sensors and actuators under the action of thermoelectromechanical loadings. To overcome the phenomenon of shear and membrane locking known in the finite-element method (FEM), a hybrid FEM model was employed [8, 9]. According to this model, the strains and resulting stresses inside a shell element are approximated separately, independently of displacements. We should note that the 6-parameter model [8] postulating a uniform distribution of transverse normal strains across the thickness of a layer package leads to the Poisson locking of shell elements in the transverse direction, while the 7-parameter one [9] is free from this drawback.

Kinematics of a Shell and Deformational Relations

Let us consider a shell consisting of N thin layers of constant thickness $h_n = z_n - z_{n-1}$, including an lth PZT piezoelectric layer of thickness h_l, where z_n is the transverse coordinate of the surface Ω_n (Fig. 1). The curvilinear orthogonal coordinates θ_1 and θ_2 are reckoned along the lines of principal curvatures, and θ_3 is the transverse coordinate. Let $\mathbf{e}_1$ and $\mathbf{e}_2$ be the unit vectors of tangents to the coordinate lines θ_1 and θ_2, and $\mathbf{e}_3$ — the unit vector of the external normal to the surface Ω. Hereinafter, the supscript n indicates that a quantity belongs to an nth layer and varies within the limits of 1 to N; $l = i_1, i_2, \ldots, i_L$ the index of a piezoelectric layer, where L is the number of piezoelectric layers attached to the external surfaces or introduced into the shell body; $\alpha, \beta = 1, 2$; $i, j = 1, 2, 3$; $A^{\mp}$ denotes a quantity belonging to the upper (+) or lower (–) surface, respectively.

The displacement field across the shell thickness is approximated according to the law [9]

$$u_\alpha = N^- u_\alpha^- + N^+ u_\alpha^+, \quad u_3 = L^- u_3^- + L^M u_3^M + L^+ u_3^+, \tag{1}$$

$$N^- = \frac{1}{h}(z^+ - \theta_3), \quad N^+ = \frac{1}{h}(\theta_3 - z^-), \tag{2}$$

$$L^- = N^-(N^- - N^+), \quad L^M = 4N^- N^+, \quad L^+ = N^+(N^+ - N^-), \tag{3}$$

where $u_i^A(\theta_1, \theta_2)$ are the tangential and transverse displacements of face surfaces Ω^- and Ω^+ of the shell; $u_3^M(\theta_1, \theta_2)$ is the transverse displacement of the midsurface Ω^M; $L^A(\theta_3)$, $L^M(\theta_3)$, and $N^A(\theta_3)$ are the Lagrange polynomials of the first and second degrees, respectively; $h = z^+ - z^-$ is the shell thickness; $z^- = z_0$ and $z^+ = z_N$ are transverse coordinates of the face surfaces.

Let us present the displacement vectors of face surfaces of the shell in the basis of reference surface:

$$\mathbf{u}^A = \sum_i u_i^A \mathbf{e}_i. \tag{4}$$

In this case, the deformation relations of the 7-parameter first-order theory of shells [9] can be written as

$$\varepsilon_{\alpha\beta} = N^- \varepsilon_{\alpha\beta}^- + N^+ \varepsilon_{\alpha\beta}^+, \quad \varepsilon_{33} = N^- \varepsilon_{33}^- + N^+ \varepsilon_{33}^+,$$
$$\varepsilon_{\alpha 3} = \varepsilon_{\alpha 3}^M, \quad \varepsilon_{\alpha 3}^M = \frac{1}{2}(\varepsilon_{\alpha 3}^- + \varepsilon_{\alpha 3}^+). \tag{5}$$

Here, $\varepsilon_{ij}^A(\theta_1, \theta_2)$ are components of the strain tensor of face surfaces of the shell:

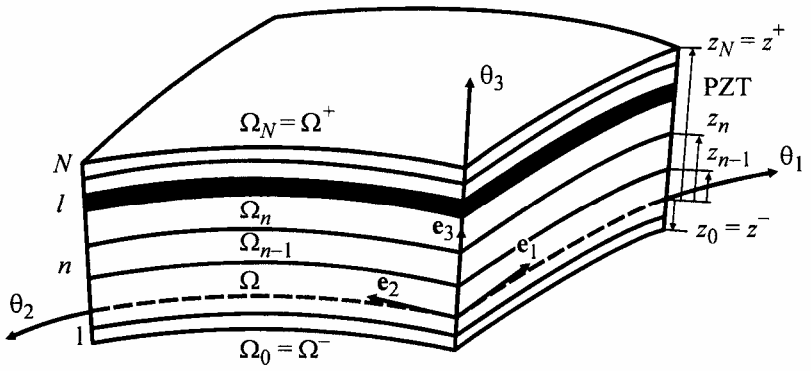

Fig. 1. Scheme of a layered shell with a piezoelectric layer (PZT).

$$2\varepsilon^{\mathrm{A}}_{\alpha\beta} = c^{\mathrm{A}}_{\alpha}\lambda^{\mathrm{A}}_{\alpha\beta} + c^{\mathrm{A}}_{\beta}\lambda^{\mathrm{A}}_{\beta\alpha},\quad \varepsilon^{\mathrm{A}}_{33} = \beta^{\mathrm{A}}_{3},\quad 2\varepsilon^{\mathrm{A}}_{\alpha 3} = c^{\mathrm{A}}_{\alpha}\beta^{\mathrm{A}}_{\alpha} + \lambda^{\mathrm{A}}_{3\alpha}, \tag{6}$$

where

$$\lambda^{\mathrm{A}}_{\alpha\alpha} = \frac{1}{A_\alpha}u^{\mathrm{A}}_{\alpha,\alpha} + B_\beta u^{\mathrm{A}}_{\beta} + k_\alpha u^{\mathrm{A}}_{3},\ \lambda^{\mathrm{A}}_{\beta\alpha} = \frac{1}{A_\alpha}u^{\mathrm{A}}_{\beta,\alpha} - B_\beta u^{\mathrm{A}}_{\alpha},\ \text{for}\ \beta \neq \alpha,$$

$$\lambda^{\mathrm{A}}_{3\alpha} = \frac{1}{A_\alpha}u^{\mathrm{A}}_{3,\alpha} - k_\alpha u^{\mathrm{A}}_{\alpha},\ \beta^{\mathrm{A}}_{\alpha} = \frac{1}{h}(u^{+}_{\alpha} - u^{-}_{\alpha}),$$

$$\beta^{-}_{3} = \frac{1}{h}(-3u^{-}_{3} + 4u^{\mathrm{M}}_{3} - u^{+}_{3}),\ \beta^{+}_{3} = \frac{1}{h}(u^{-}_{3} - 4u^{\mathrm{M}}_{3} + 3u^{+}_{3}), \tag{7}$$

$$c^{\mathrm{A}}_{\alpha} = 1 + k_\alpha z^{\mathrm{A}},\quad B_\alpha = \frac{1}{A_\alpha A_\beta}A_{\beta,\alpha}\quad \text{for}\ \beta \neq \alpha;$$

A_α and k_α are the Lamé parameters and the principal curvatures of the reference surface; c^{A}_{α} are shear components on the face surfaces of the shell; the symbol $(\ )_{,\alpha}$ means a particular derivative along the coordinate θ_α. It can be shown that deformation relations (5) and (6) exactly represent solid-body displacements of the shell in the system of curvilinear coordinates of reference surface [10].

Description of Electric and Temperature Fields

We assume that the electric potential is distributed across the thickness of layer package according to the broken-line hypothesis [11, 12]:

$$\varphi = \sum_n (\overline{N}^{-}_{n}\varphi_{n-1} + \overline{N}^{+}_{n}\varphi_{n}),\quad \overline{N}^{\mathrm{A}}_{n} = \begin{cases} N^{\mathrm{A}}_{n}, & \theta_3 \in [z_{n-1}, z_n] \\ 0, & \theta_3 \notin [z_{n-1}, z_n] \end{cases}, \tag{8}$$

$$N_n^- = \frac{1}{h_n}(z_n - \theta_3), \quad N_n^+ = \frac{1}{h_n}(\theta_3 - z_{n-1}), \quad \theta_3 \in [z_{n-1}, z_n], \tag{8}$$

where $\varphi_{n-1}(\theta_1, \theta_2)$ and $\varphi_n(\theta_1, \theta_2)$ are values of the electric potential on the lower and upper surfaces of an nth layer.

The relation between the vector of electric field intensity $\mathbf{E}$ and the electric potential φ is found by the equation known in electrostatics

$$\mathbf{E} = -\nabla\varphi. \tag{9}$$

Thus, the vector of electric field intensity has the following distribution across the thickness of an nth layer:

$$E_\alpha^{(n)} = N_n^- E_\alpha^{(n)-} + N_n^+ E_\alpha^{(n)+}, \quad E_3^{(n)} = -\frac{1}{h_n}(\varphi_n - \varphi_{n-1}),$$
$$E_\alpha^{(n)-} = -\frac{1}{A_\alpha}\varphi_{n-1,\alpha}, \quad E_\alpha^{(n)+} = -\frac{1}{A_\alpha}\varphi_{n,\alpha}, \tag{10}$$

where $E_i^{(n)}$ are the tangential and transverse components of the vector of electric field intensity of the nth layer. As seen, the transverse component $E_3^{(n)}$ is constant across the thickness of a piezoelectric layer; however, this fact does not impose significant restrictions on an analysis of piezoelectric shells. If necessary, by splitting the piezoelectric layer into several fictitious layers, results acceptable in practical applications can be achieved.

For the temperature field, we will use the same approximation:

$$\Theta = \sum_n (\overline{N}_n^- \Theta_{n-1} + \overline{N}_n^+ \Theta_n), \tag{11}$$

where $\Theta = T - T_0$ is the temperature increment relative to the natural state; T_0 is the Kelvin temperature of the natural state; $\Theta_{n-1}(\theta_1, \theta_2)$ and $\Theta_n(\theta_1, \theta_2)$ are temperatures on the external surfaces of an nth layer.

Equations of Thermoelectroelasticity

The state equations of the linear theory of thermoelectroelasticity for an lth piezoelectric layer belonging to the monoclinic system of symmetry class 2, in the presence of a binary axis parallel to the transverse coordinate, can be written in the form [13]

$$\boldsymbol{\varepsilon} = \mathbf{A}^{(l)}\boldsymbol{\sigma}^{(l)} + (\mathbf{d}^{(l)})^T \mathbf{E}^{(l)} + \boldsymbol{\alpha}^{(l)}\Theta, \tag{12}$$

$$\mathbf{D}^{(l)} = \mathbf{d}^{(l)}\boldsymbol{\sigma}^{(l)} + \boldsymbol{\zeta}^{(l)}\mathbf{E}^{(l)} + \boldsymbol{\eta}^{(l)}\Theta, \tag{13}$$

where $\boldsymbol{\varepsilon}$ is the strain vector; $\boldsymbol{\sigma}^{(l)}$ is the stress vector; $\mathbf{E}^{(l)}$ is the vector of electric field intensity; $\mathbf{D}^{(l)}$ is the electric displacement vector; $\mathbf{A}^{(l)}$ is the compliance matrix; $\mathbf{d}^{(l)}$ is the matrix of piezoelectric constants; $\boldsymbol{\zeta}^{(l)}$ is the matrix of dielectric constants; $\boldsymbol{\alpha}^{(l)}$ is the vector of thermal expansion coefficients and shear; $\boldsymbol{\eta}^{(l)}$ is the vector of pyroelectric constants:

$$\boldsymbol{\varepsilon} = [\varepsilon_{11}\ \varepsilon_{22}\ \varepsilon_{33}\ 2\varepsilon_{23}\ 2\varepsilon_{13}\ 2\varepsilon_{12}]^T, \quad \boldsymbol{\sigma}^{(l)} = [\sigma_{11}^{(l)}\ \sigma_{22}^{(l)}\ \sigma_{33}^{(l)}\ \sigma_{23}^{(l)}\ \sigma_{13}^{(l)}\ \sigma_{12}^{(l)}]^T,$$
$$\mathbf{E}^{(l)} = [E_1^{(l)}\ E_2^{(l)}\ E_3^{(l)}]^T, \quad \mathbf{D}^{(l)} = [D_1^{(l)}\ D_2^{(l)}\ D_3^{(l)}]^T, \tag{14}$$

$$\mathbf{A}^{(l)} = \begin{bmatrix} A_{11}^{(l)} & A_{12}^{(l)} & A_{13}^{(l)} & 0 & 0 & A_{16}^{(l)} \\ & A_{22}^{(l)} & A_{23}^{(l)} & 0 & 0 & A_{26}^{(l)} \\ & & A_{33}^{(l)} & 0 & 0 & A_{36}^{(l)} \\ & & & A_{44}^{(l)} & A_{45}^{(l)} & 0 \\ & & & & A_{55}^{(l)} & 0 \\ \text{sym} & & & & & A_{66}^{(l)} \end{bmatrix}, \tag{14}$$

$$\mathbf{d}^{(l)} = \begin{bmatrix} 0 & 0 & 0 & d_{14}^{(l)} & d_{15}^{(l)} & 0 \\ 0 & 0 & 0 & d_{24}^{(l)} & d_{25}^{(l)} & 0 \\ d_{31}^{(l)} & d_{32}^{(l)} & d_{33}^{(l)} & 0 & 0 & d_{36}^{(l)} \end{bmatrix}, \quad \zeta^{(l)} = \begin{bmatrix} \zeta_{11}^{(l)} & \zeta_{12}^{(l)} & 0 \\ & \zeta_{22}^{(l)} & 0 \\ \text{sym} & & \zeta_{33}^{(l)} \end{bmatrix},$$

$$\boldsymbol{\alpha}^{(l)} = [\alpha_1^{(l)} \; \alpha_2^{(l)} \; \alpha_3^{(l)} \; 0 \; 0 \; 2\alpha_6^{(l)}]^T, \quad \boldsymbol{\eta}^{(l)} = [0 \; 0 \; \eta_3^{(l)}]^T.$$

Solving Eq. (12) for the stress vector and inserting the latter into state equation (13) yields

$$\boldsymbol{\sigma}^{(l)} = \mathbf{C}^{(l)}\boldsymbol{\varepsilon} - (\mathbf{e}^{(l)})^T \mathbf{E}^{(l)} - \boldsymbol{\gamma}^{(l)}\Theta, \tag{15}$$

$$\mathbf{D}^{(l)} = \mathbf{e}^{(l)}\boldsymbol{\varepsilon} + \in^{(l)} \mathbf{E}^{(l)} + \mathbf{g}^{(l)}\Theta, \tag{16}$$

where $\mathbf{C}^{(l)}$ is the material stiffness matrix; $\mathbf{e}^{(l)}$ and $\in^{(l)}$ are the piezoelectric and dielectric matrices; $\boldsymbol{\gamma}^{(l)}$ is the vector of temperature stresses; $\mathbf{g}^{(l)}$ is the vector of pyroelectric constants:

$$\mathbf{C}^{(l)} = (\mathbf{A}^{(l)})^{-1}, \quad \mathbf{e}^{(l)} = \mathbf{d}^{(l)}\mathbf{C}^{(l)}, \quad \in^{(l)} = \zeta^{(l)} - \mathbf{d}^{(l)}\mathbf{C}^{(l)}(\mathbf{d}^{(l)})^T,$$
$$\boldsymbol{\gamma}^{(l)} = \mathbf{C}^{(l)}\boldsymbol{\alpha}^{(l)}, \quad \mathbf{g}^{(l)} = \boldsymbol{\eta}^{(l)} - \mathbf{d}^{(l)}\mathbf{C}^{(l)}\boldsymbol{\alpha}^{(l)}. \tag{17}$$

Combined Variational Equation for Calculating a Layered Thermoelectroelastic Shell

The 7-parameter first-order theory of thermopiezoelectric shells suggested is based on approximations of displacements (1), strains (5), electric potential (8), and the vector of electric field intensity (10) and temperature (11) in the transverse direction. We will also introduce the approximations, agreed with (5), for the strains independent of the displacement field

$$\hat{\varepsilon}_{\alpha\beta} = N^- \hat{\varepsilon}_{\alpha\beta}^- + N^+ \hat{\varepsilon}_{\alpha\beta}^+, \quad \hat{\varepsilon}_{33} = N^- \hat{\varepsilon}_{33}^- + N^+ \hat{\varepsilon}_{33}^+, \quad \hat{\varepsilon}_{\alpha 3} = \hat{\varepsilon}_{\alpha 3}^{\mathrm{M}}, \tag{18}$$

where $\hat{\varepsilon}_{\alpha\beta}^{\mathrm{A}}(\theta_1, \theta_2)$ and $\hat{\varepsilon}_{33}^{\mathrm{A}}(\theta_1, \theta_2)$ are the independently introduced tangential and transverse normal strains of external surfaces of the shell, and $\hat{\varepsilon}_{\alpha 3}^{\mathrm{M}}(\theta_1, \theta_2)$ are the independently introduced transverse shear strains of midsurface.

Let us now insert approximations (1), (5), (8), (10), (11), and (18) into the mixed variational equation of the 3-D theory of thermopiezoelectricity [13, 14]. Introducing the resulting stresses

$$H_{\alpha\beta}^{\mathrm{A}} = \sum_n \int_{z_{n-1}}^{z_n} \sigma_{\alpha\beta}^{(n)} N^{\mathrm{A}} d\theta_3, \quad H_{33}^{\mathrm{A}} = \sum_n \int_{z_{n-1}}^{z_n} \sigma_{33}^{(n)} N^{\mathrm{A}} d\theta_3, \quad H_{\alpha 3} = \sum_n \int_{z_{n-1}}^{z_n} \sigma_{\alpha 3}^{(n)} d\theta_3 \tag{19}$$

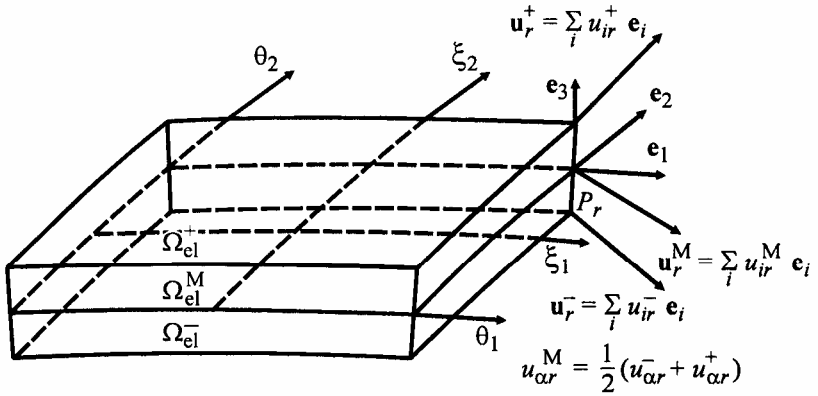

Fig. 2. Geometrically exact piezoelectric element of the shell on the basis of a 7-parameter model. P_r is the nodal point ($r = 1, 2, 3, 4$).

and assuming that the metric of surfaces parallel to the reference one are equal to that of midsurface, we come to the Hu–Washizu variational principle for the 7-parameter thermopiezoelectric shell element

$$\int_{-1}^{1}\int_{-1}^{1}[\delta\hat{\boldsymbol{\varepsilon}}^T(\mathbf{H}-\mathbf{D}_{uu}\hat{\boldsymbol{\varepsilon}}+\mathbf{D}_{u\varphi}\tilde{\mathbf{E}}+\mathbf{D}_{u\theta}\boldsymbol{\Psi})+\delta\tilde{\mathbf{E}}^T(\mathbf{D}_{\varphi u}\hat{\boldsymbol{\varepsilon}}+\mathbf{D}_{\varphi\varphi}\tilde{\mathbf{E}}+\mathbf{D}_{\varphi\theta}\boldsymbol{\Psi})$$

$$+\delta\mathbf{H}^T(\hat{\boldsymbol{\varepsilon}}-\tilde{\boldsymbol{\varepsilon}})-\delta\tilde{\boldsymbol{\varepsilon}}^T\mathbf{H}+\delta\mathbf{v}^T\mathbf{p}+\delta\boldsymbol{\chi}^T\mathbf{q}]A_1A_2c_1^Mc_2^Ml_1l_2d\xi_1d\xi_2=0. \tag{20}$$

Here, $\xi_\alpha=(\theta_\alpha-d_\alpha)/l_\alpha$ are the normalized curvilinear coordinates of the shell element (Fig. 2); d_α are center coordinates of the element; $2l_\alpha$ is its length in the θ_α-direction; $c_\alpha^M=1+k_\alpha z^M$ are shear components on the shell midsurface; $z^M=(z^-+z^+)/2$ is the transverse coordinate of the midsurface Ω^M; $\mathbf{v}$ is the displacement vector of external surfaces; $\tilde{\boldsymbol{\varepsilon}}$ and $\hat{\boldsymbol{\varepsilon}}$ are the strain vectors of external surfaces dependent and independent of the field of displacements; $\mathbf{H}$ is the vector of resulting stresses (19); $\boldsymbol{\chi}$ and $\boldsymbol{\Psi}$ are the vectors of electric potentials and temperatures on external surfaces of the shell and on interfaces; $\tilde{\mathbf{E}}$ is the vector of electric field intensity; $\mathbf{p}$ is the vector of surface load; $\mathbf{q}$ is the vector of surface charges on external surfaces of the shell and on layer interfaces; $\mathbf{D}_{uu}$, $\mathbf{D}_{u\varphi}$, and $\mathbf{D}_{\varphi\varphi}$ are the mechanical, piezoelectric, and dielectric matrices; $\mathbf{D}_{u\theta}$ is the matrix of thermal stiffness; $\mathbf{D}_{\varphi\theta}$ is the pyroelectric matrix:

$$\mathbf{v}=[u_1^-\ u_2^-\ u_3^-\ u_1^+\ u_2^+\ u_3^+\ u_3^M]^T,$$

$$\tilde{\boldsymbol{\varepsilon}}=[\varepsilon_{11}^-\ \varepsilon_{11}^+\ \varepsilon_{22}^-\ \varepsilon_{22}^+\ \varepsilon_{33}^-\ \varepsilon_{33}^+\ 2\varepsilon_{12}^-\ 2\varepsilon_{12}^+\ 2\varepsilon_{13}^M\ 2\varepsilon_{23}^M]^T,$$

$$\hat{\boldsymbol{\varepsilon}}=[\hat{\varepsilon}_{11}^-\ \hat{\varepsilon}_{11}^+\ \hat{\varepsilon}_{22}^-\ \hat{\varepsilon}_{22}^+\ \hat{\varepsilon}_{33}^-\ \hat{\varepsilon}_{33}^+\ 2\hat{\varepsilon}_{12}^-\ 2\hat{\varepsilon}_{12}^+\ 2\hat{\varepsilon}_{13}^M\ 2\hat{\varepsilon}_{23}^M]^T, \tag{21}$$

$$\mathbf{H}=[H_{11}^-\ H_{11}^+\ H_{22}^-\ H_{22}^+\ H_{33}^-\ H_{33}^+\ H_{12}^-\ H_{12}^+\ H_{13}\ H_{23}]^T,$$

$$\boldsymbol{\chi}=[\varphi_0\ \varphi_1\ldots\varphi_N]^T,\quad \boldsymbol{\Psi}=[\Theta_0\ \Theta_1\ldots\Theta_N]^T,$$

$$\tilde{\mathbf{E}}=[(\tilde{\mathbf{E}}^{(1)})^T\ (\tilde{\mathbf{E}}^{(2)})^T\ldots(\tilde{\mathbf{E}}^{(N)})^T]^T,\quad \tilde{\mathbf{E}}^{(n)}=[E_1^{(n)-}\ E_1^{(n)+}\ E_2^{(n)-}\ E_2^{(n)+}\ E_3^{(n)}]^T,$$

$$\mathbf{p}=[-p_1^- \; -p_2^- \; -p_3^- \; p_1^+ \; p_2^+ \; p_3^+ \; 0]^T, \quad \mathbf{q}=[q_s^{(0)} \; q_s^{(1)} \ldots q_s^{(N)}]^T,$$

$$\mathbf{D}_{uu}=\begin{bmatrix}
D_{11}^{00} & D_{11}^{01} & D_{12}^{00} & D_{12}^{01} & D_{13}^{00} & D_{13}^{01} & D_{16}^{00} & D_{16}^{01} & 0 & 0 \\
 & D_{11}^{11} & D_{12}^{01} & D_{12}^{11} & D_{13}^{01} & D_{13}^{11} & D_{16}^{01} & D_{16}^{11} & 0 & 0 \\
 & & D_{22}^{00} & D_{22}^{01} & D_{23}^{00} & D_{23}^{01} & D_{26}^{00} & D_{26}^{01} & 0 & 0 \\
 & & & D_{22}^{11} & D_{23}^{01} & D_{23}^{11} & D_{26}^{01} & D_{26}^{11} & 0 & 0 \\
 & & & & D_{33}^{00} & D_{33}^{01} & D_{36}^{00} & D_{36}^{01} & 0 & 0 \\
 & & & & & D_{33}^{11} & D_{36}^{01} & D_{36}^{11} & 0 & 0 \\
 & & & & & & D_{66}^{00} & D_{66}^{01} & 0 & 0 \\
 & & & & & & & D_{66}^{11} & 0 & 0 \\
 & & & & & & & & D_{55} & D_{45} \\
\text{sym} & & & & & & & & & D_{44}
\end{bmatrix},$$

$$\mathbf{D}_{u\varphi}=[\mathbf{D}_{u\varphi}^{(1)} \; \mathbf{D}_{u\varphi}^{(2)} \ldots \mathbf{D}_{u\varphi}^{(N)}], \quad \mathbf{D}_{\varphi u}=\mathbf{D}_{u\varphi}^T,$$

$$\mathbf{D}_{u\varphi}^{(n)}=\begin{bmatrix}
0 & 0 & 0 & 0 & m_n^0 e_{31}^{(n)} \\
0 & 0 & 0 & 0 & m_n^1 e_{31}^{(n)} \\
0 & 0 & 0 & 0 & m_n^0 e_{32}^{(n)} \\
0 & 0 & 0 & 0 & m_n^1 e_{32}^{(n)} \\
0 & 0 & 0 & 0 & m_n^0 e_{33}^{(n)} \\
0 & 0 & 0 & 0 & m_n^1 e_{33}^{(n)} \\
0 & 0 & 0 & 0 & m_n^0 e_{36}^{(n)} \\
0 & 0 & 0 & 0 & m_n^1 e_{36}^{(n)} \\
k_n^0 e_{15}^{(n)} & k_n^1 e_{15}^{(n)} & k_n^0 e_{25}^{(n)} & k_n^1 e_{25}^{(n)} & 0 \\
k_n^0 e_{14}^{(n)} & k_n^1 e_{14}^{(n)} & k_n^0 e_{24}^{(n)} & k_n^1 e_{24}^{(n)} & 0
\end{bmatrix}, \tag{21}$$

$$\mathbf{D}_{u\theta}=\begin{bmatrix}
l_1^{00}\gamma_1^{(1)} & l_1^{01}\gamma_1^{(1)}+l_2^{00}\gamma_1^{(2)} & \ldots & l_{N-1}^{01}\gamma_1^{(N-1)}+l_N^{00}\gamma_1^{(N)} & l_N^{01}\gamma_1^{(N)} \\
l_1^{10}\gamma_1^{(1)} & l_1^{11}\gamma_1^{(1)}+l_2^{10}\gamma_1^{(2)} & \ldots & l_{N-1}^{11}\gamma_1^{(N-1)}+l_N^{10}\gamma_1^{(N)} & l_N^{11}\gamma_1^{(N)} \\
l_1^{00}\gamma_2^{(1)} & l_1^{01}\gamma_2^{(1)}+l_2^{00}\gamma_2^{(2)} & \ldots & l_{N-1}^{01}\gamma_2^{(N-1)}+l_N^{00}\gamma_2^{(N)} & l_N^{01}\gamma_2^{(N)} \\
l_1^{10}\gamma_2^{(1)} & l_1^{11}\gamma_2^{(1)}+l_2^{10}\gamma_2^{(2)} & \ldots & l_{N-1}^{11}\gamma_2^{(N-1)}+l_N^{10}\gamma_2^{(N)} & l_N^{11}\gamma_2^{(N)} \\
l_1^{00}\gamma_3^{(1)} & l_1^{01}\gamma_3^{(1)}+l_2^{00}\gamma_3^{(2)} & \ldots & l_{N-1}^{01}\gamma_3^{(N-1)}+l_N^{00}\gamma_3^{(N)} & l_N^{01}\gamma_3^{(N)} \\
l_1^{10}\gamma_3^{(1)} & l_1^{11}\gamma_3^{(1)}+l_2^{10}\gamma_3^{(2)} & \ldots & l_{N-1}^{11}\gamma_3^{(N-1)}+l_N^{10}\gamma_3^{(N)} & l_N^{11}\gamma_3^{(N)} \\
l_1^{00}\gamma_6^{(1)} & l_1^{01}\gamma_6^{(1)}+l_2^{00}\gamma_6^{(2)} & \ldots & l_{N-1}^{01}\gamma_6^{(N-1)}+l_N^{00}\gamma_6^{(N)} & l_N^{01}\gamma_6^{(N)} \\
l_1^{10}\gamma_6^{(1)} & l_1^{11}\gamma_6^{(1)}+l_2^{10}\gamma_6^{(2)} & \ldots & l_{N-1}^{11}\gamma_6^{(N-1)}+l_N^{10}\gamma_6^{(N)} & l_N^{11}\gamma_6^{(N)} \\
0 & 0 & \ldots & 0 & 0 \\
0 & 0 & \ldots & 0 & 0
\end{bmatrix},$$

$$\mathbf{D}_{\varphi\varphi} = \begin{bmatrix} \mathbf{D}_{\varphi\varphi}^{(1)} & \mathbf{0}_{5\times5} & \dots & \mathbf{0}_{5\times5} \\ \mathbf{0}_{5\times5} & \mathbf{D}_{\varphi\varphi}^{(2)} & \dots & \mathbf{0}_{5\times5} \\ \dots & & & \\ \mathbf{0}_{5\times5} & \mathbf{0}_{5\times5} & \dots & \mathbf{D}_{\varphi\varphi}^{(N)} \end{bmatrix},$$

$$\mathbf{D}_{\varphi\varphi}^{(n)} = \begin{bmatrix} k_n^{00}\in_{11}^{(n)} & k_n^{01}\in_{11}^{(n)} & k_n^{00}\in_{12}^{(n)} & k_n^{01}\in_{12}^{(n)} & 0 \\ & k_n^{11}\in_{11}^{(n)} & k_n^{01}\in_{12}^{(n)} & k_n^{11}\in_{12}^{(n)} & 0 \\ & & k_n^{00}\in_{22}^{(n)} & k_n^{01}\in_{22}^{(n)} & 0 \\ & & & k_n^{11}\in_{22}^{(n)} & 0 \\ \text{sym} & & & & h_n\in_{33}^{(n)} \end{bmatrix}, \tag{21}$$

$$\mathbf{D}_{\varphi\theta} = \begin{bmatrix} \mathbf{D}_{\varphi\theta}^{(1)} & \mathbf{D}_{\varphi\theta}^{(1)} & \mathbf{0}_{5\times1} & \dots & \mathbf{0}_{5\times1} & \mathbf{0}_{5\times1} \\ \mathbf{0}_{5\times1} & \mathbf{D}_{\varphi\theta}^{(2)} & \mathbf{D}_{\varphi\theta}^{(2)} & \dots & \mathbf{0}_{5\times1} & \mathbf{0}_{5\times1} \\ \dots & & & & & \\ \mathbf{0}_{5\times1} & \mathbf{0}_{5\times1} & \mathbf{0}_{5\times1} & \dots & \mathbf{D}_{\varphi\theta}^{(N)} & \mathbf{D}_{\varphi\theta}^{(N)} \end{bmatrix},$$

$$\mathbf{D}_{\varphi\theta}^{(n)} = [0000h_n g_3^{(n)}/2]^T,$$

where p_i^{A} are the surface loads operating on the external surfaces in the θ_i-directions; $q_s^{(n-1)}$ and $q_s^{(n)}$ are densities of the surface charge on the surfaces Ω_{n-1} and Ω_n. Also, we introduced the additional designations

$$D_{ab}^{pq} = \sum_n m_n^{pq} C_{ab}^{(n)}, \quad D_{cd} = \sum_n h_n C_{cd}^{(n)},$$

$$m_n^{pq} = \int_{z_{n-1}}^{z_n} (N^-)^{2-p-q} (N^+)^{p+q}\, d\theta_3, \quad m_n^p = \int_{z_{n-1}}^{z_n} (N^-)^{1-p} (N^+)^p\, d\theta_3, \tag{22}$$

$$k_n^{pq} = \int_{z_{n-1}}^{z_n} (N_n^-)^{2-p-q} (N_n^+)^{p+q}\, d\theta_3, \quad k_n^p = \int_{z_{n-1}}^{z_n} (N_n^-)^{1-p} (N_n^+)^p\, d\theta_3 = \frac{1}{2} h_n,$$

$$l_n^{pq} = \int_{z_{n-1}}^{z_n} (N^-)^{1-p} (N^+)^p (N_n^-)^{1-q} (N_n^+)^q\, d\theta_3,$$

where $a, b = 1, 2, 3, 6$; $c, d = 4, 5$; $p, q = 0, 1$.

Note 1. In variational equation (20), the independent functional variables are $\mathbf{v}$, $\hat{\boldsymbol{\varepsilon}}$, $\mathbf{H}$, and $\boldsymbol{\chi}$. Since the strain vector $\tilde{\boldsymbol{\varepsilon}}$ and the vector of electric field intensity $\tilde{\mathbf{E}}$ are dependent quantities, their variations can be found by the formulas

$$\delta\tilde{\boldsymbol{\varepsilon}} = \frac{\partial\tilde{\boldsymbol{\varepsilon}}}{\partial\mathbf{v}}\delta\mathbf{v}, \quad \delta\tilde{\mathbf{E}} = \frac{\partial\tilde{\mathbf{E}}}{\partial\varphi}\delta\varphi. \tag{23}$$

We should also note that the electric displacement vector $\mathbf{D}^{(l)}$ is excluded from the Hu–Washizu variational equation (20), which allows us to simplify the finite-element formulation.

Note 2. In the case of stationary processes of the theory of thermopiezoelectricity, the equation of heat conductivity is not connected with the other equations [13]. Thus, it is possible to reduce the number of independent variables assuming that the vector Ψ is given.

Geometrically Exact Hybrid Element of a Thermopiezoelectric Shell

The finite-element formulation for a geometrically exact four-node thermopiezoelectric shell element is based on a simple and effective bilinear interpolation of displacements, electric potential, and temperature:

$$\mathbf{v}=\sum_r N_r \mathbf{v}_r\,,\quad \mathbf{v}_r=[u_{1r}^{-}\ u_{2r}^{-}\ u_{3r}^{-}\ u_{1r}^{+}\ u_{2r}^{+}\ u_{3r}^{+}\ u_{3r}^{\mathrm{M}}]^T, \tag{24}$$

$$\chi=\sum_r N_r \chi_r,\quad \chi_r=[\varphi_{0r}\ \varphi_{1r}\dots\varphi_{Nr}]^T, \tag{25}$$

$$\Psi=\sum_r N_r \Psi_r,\quad \Psi_r=[\Theta_{0r}\ \Theta_{1r}\dots\Theta_{Nr}]^T, \tag{26}$$

where $N_r(\xi_1,\xi_2)$ are bilinear functions of element form; $\mathbf{v}_r$, χ_r, and Ψ_r are the vectors of displacements, electric potential, and temperature at nodes of the element; the subscript r stands for the node number and varies from 1 to 4.

To perform an analytical integration within the limits of the element, we again use a bilinear interpolation [12, 15] for the strain vector and the vector of electric field intensity:

$$\tilde{\varepsilon}=\sum_r N_r \tilde{\varepsilon}_r,\quad \varepsilon_r=\tilde{\varepsilon}(\mathbf{P}_r)=\mathbf{B}_r^u\mathbf{U}, \tag{27}$$

$$\tilde{\mathbf{E}}=\sum_r N_r \tilde{\mathbf{E}}_r,\quad \tilde{\mathbf{E}}_r=\tilde{\mathbf{E}}(\mathbf{P}_r)=-\mathbf{B}_r^{\varphi}\Phi, \tag{28}$$

where $\mathbf{B}_r^u$ and $\mathbf{B}_r^{\varphi}$ are 10×28 and $5N\times 4(N+1)$ matrices *constant on the element*; $\mathbf{U}$ is the vector of nodal displacements; Φ is the vector of nodal values of the electric potential:

$$\mathbf{U}=[\mathbf{v}_1^T\ \mathbf{v}_2^T\ \mathbf{v}_3^T\ \mathbf{v}_4^T]^T,\quad \Phi=[\chi_1^T\ \chi_2^T\ \chi_3^T\ \chi_4^T]^T. \tag{29}$$

To simplify the calculation process, interpolations (26)-(28) are conveniently presented in the form

$$\tilde{\varepsilon}=\sum_{r_1,r_2}(\xi_1)^{r_1}\ (\xi_2)^{r_2}\tilde{\varepsilon}^{r_1r_2},\quad \tilde{\varepsilon}^{r_1r_2}=\mathbf{B}_u^{r_1r_2}\mathbf{U}, \tag{30}$$

$$\tilde{\mathbf{E}}=\sum_{r_1,r_2}(\xi_1)^{r_1}\ (\xi_2)^{r_2}\tilde{\mathbf{E}}^{r_1r_2},\quad \tilde{\mathbf{E}}^{r_1r_2}=-\mathbf{B}_{\varphi}^{r_1r_2}\Phi, \tag{31}$$

$$\Psi=\sum_{r_1,r_2}(\xi_1)^{r_1}\ (\xi_2)^{r_2}\Psi^{r_1r_2}, \tag{32}$$

where

$$\mathbf{B}_u^{00}=\frac{1}{4}(\mathbf{B}_1^u+\mathbf{B}_2^u+\mathbf{B}_3^u+\mathbf{B}_4^u),\quad \mathbf{B}_u^{01}=\frac{1}{4}(\mathbf{B}_1^u+\mathbf{B}_2^u-\mathbf{B}_3^u-\mathbf{B}_4^u), \tag{33}$$

$$\mathbf{B}_u^{10} = \frac{1}{4}(\mathbf{B}_1^u - \mathbf{B}_2^u - \mathbf{B}_3^u + \mathbf{B}_4^u), \quad \mathbf{B}_u^{11} = \frac{1}{4}(\mathbf{B}_1^u - \mathbf{B}_2^u + \mathbf{B}_3^u - \mathbf{B}_4^u). \tag{33}$$

The matrices $\mathbf{B}_\varphi^{r_1 r_2}$ and columns $\Psi^{r_1 r_2}$ are calculated in a similar way by using the matrices $\mathbf{B}_r^\varphi$ and columns Ψ_r, respectively; hereinafter, the subscripts r_1 and r_2 take the values 0 and 1.

To avoid the shear and membrane locking of shell elements and the rise of false energy modes, we use the following approximations [9, 15] for the independently introduced strains and resulting stresses:

$$\hat{\boldsymbol{\varepsilon}} = \sum_{r_1, r_2} (\xi_1)^{r_1} (\xi_2)^{r_2} \mathbf{Q}^{r_1 r_2} \hat{\boldsymbol{\varepsilon}}^{r_1 r_2},$$

$$\hat{\boldsymbol{\varepsilon}}^{00} = [\hat{\varepsilon}_{11}^{-00}\ \hat{\varepsilon}_{11}^{+00}\ \hat{\varepsilon}_{22}^{-00}\ \hat{\varepsilon}_{22}^{+00}\ \hat{\varepsilon}_{33}^{-00}\ \hat{\varepsilon}_{33}^{+00}\ 2\hat{\varepsilon}_{12}^{-00}\ 2\hat{\varepsilon}_{12}^{+00}\ 2\hat{\varepsilon}_{13}^{M00}\ 2\hat{\varepsilon}_{23}^{M00}]^T, \tag{34}$$

$$\hat{\boldsymbol{\varepsilon}}^{01} = [\hat{\varepsilon}_{11}^{-01}\ \hat{\varepsilon}_{11}^{+01}\ \hat{\varepsilon}_{33}^{-01}\ \hat{\varepsilon}_{33}^{+01}\ 2\hat{\varepsilon}_{13}^{M01}]^T, \quad \hat{\boldsymbol{\varepsilon}}^{10} = [\hat{\varepsilon}_{22}^{-10}\ \hat{\varepsilon}_{22}^{+10}\ \hat{\varepsilon}_{33}^{-10}\ \hat{\varepsilon}_{33}^{+10}\ 2\hat{\varepsilon}_{23}^{M10}]^T,$$

$$\hat{\boldsymbol{\varepsilon}}^{11} = [\hat{\varepsilon}_{33}^{-11}\ \hat{\varepsilon}_{33}^{+11}]^T,$$

$$\mathbf{H} = \sum_{r_1, r_2} (\xi_1)^{r_1} (\xi_2)^{r_2} \mathbf{Q}^{r_1 r_2} \mathbf{H}^{r_1 r_2},$$

$$\mathbf{H}^{00} = [H_{11}^{-00}\ H_{11}^{+00}\ H_{22}^{-00}\ H_{22}^{+00}\ H_{33}^{-00}\ H_{33}^{+00}\ H_{12}^{-00}\ H_{12}^{+00}\ H_{13}^{00}\ H_{23}^{00}]^T, \tag{35}$$

$$\mathbf{H}^{01} = [H_{11}^{-01}\ H_{11}^{+01}\ H_{33}^{-01}\ H_{33}^{+01}\ H_{13}^{01}]^T,$$

$$\mathbf{H}^{10} = [H_{22}^{-10}\ H_{22}^{+10}\ H_{33}^{-10}\ H_{33}^{+10}\ H_{23}^{10}]^T, \quad \mathbf{H}^{11} = [H_{33}^{-11}\ H_{33}^{+11}]^T,$$

where $\mathbf{Q}^{00}$ is the 10×10 unit matrix; $\mathbf{Q}^{01}$ and $\mathbf{Q}^{10}$ are 10×5 projection matrices; $\mathbf{Q}^{11}$ is a 10×2 projection matrix [9, 15].

Inserting interpolations (24), (25), (30)-(32), (34), and (35) in the mixed variational equation (20), performing an analytical integration within the limits of the element, and excluding the independently introduced strains $\hat{\boldsymbol{\varepsilon}}^{r_1 r_2}$ and the resulting stresses $\mathbf{H}^{r_1 r_2}$, we arrive at the equilibrium equations of the element

$$\begin{bmatrix} \mathbf{K}_{uu} & \mathbf{K}_{u\varphi} \\ \mathbf{K}_{\varphi u} & \mathbf{K}_{\varphi\varphi} \end{bmatrix} \begin{bmatrix} \mathbf{U} \\ \boldsymbol{\Phi} \end{bmatrix} = \begin{bmatrix} \mathbf{F}_p + \mathbf{F}_{u\theta} \\ \mathbf{F}_q + \mathbf{F}_{\varphi\theta} \end{bmatrix}, \tag{36}$$

where $\mathbf{K}_{uu}$, $\mathbf{K}_{u\varphi}$, and $\mathbf{K}_{\varphi\varphi}$ are the matrices of mechanical, piezoelectric, and dielectric stiffnesses; $\mathbf{F}_p$ is the vector of surface loads; $\mathbf{F}_q$ is the vector of electric loading; $\mathbf{F}_{u\theta}$ and $\mathbf{F}_{\varphi\theta}$ are the vectors of thermal loading:

$$\mathbf{K}_{uu} = \sum_{r_1, r_2} \frac{1}{3^{r_1 + r_2}} (\mathbf{B}_u^{r_1 r_2})^T \mathbf{Q}^{r_1 r_2} (\mathbf{Q}^{r_1 r_2})^T \mathbf{D}_{uu} \mathbf{Q}^{r_1 r_2} (\mathbf{Q}^{r_1 r_2})^T \mathbf{B}_u^{r_1 r_2},$$

$$\mathbf{K}_{u\varphi} = \sum_{r_1, r_2} \frac{1}{3^{r_1 + r_2}} (\mathbf{B}_u^{r_1 r_2})^T \mathbf{Q}^{r_1 r_2} (\mathbf{Q}^{r_1 r_2})^T \mathbf{D}_{u\varphi} \mathbf{B}_\varphi^{r_1 r_2}, \quad \mathbf{K}_{\varphi u} = (\mathbf{K}_{u\varphi})^T, \tag{37}$$

$$\mathbf{K}_{\varphi\varphi} = -\sum_{r_1, r_2} \frac{1}{3^{r_1 + r_2}} (\mathbf{B}_\varphi^{r_1 r_2})^T \mathbf{D}_{\varphi\varphi} \mathbf{B}_\varphi^{r_1 r_2},$$

$$\mathbf{F}_{u\theta} = -\sum_{r_1,r_2} \frac{1}{3^{r_1+r_2}} (\mathbf{B}_u^{r_1 r_2})^T \mathbf{Q}^{r_1 r_2} (\mathbf{Q}^{r_1 r_2})^T \mathbf{D}_{u\theta} \boldsymbol{\Psi}^{r_1 r_2},$$

$$\mathbf{F}_{\varphi\theta} = -\sum_{r_1,r_2} \frac{1}{3^{r_1+r_2}} (\mathbf{B}_\varphi^{r_1 r_2})^T \mathbf{D}_{\varphi\theta} \boldsymbol{\Psi}^{r_1 r_2}. \tag{37}$$

Note 3. To deduce the system of equations (36), a numerical inversion of matrices is not necessary, which is not typical of isoparametric hybrid shell elements. Attention is also called to the use of analytical integration, which additionally ensures the calculation efficiency of the geometrically exact thermopiezoelectric shell element developed.

Each interface of layers can be considered either active (with a known electric potential) or sensorial (with an unknown electric potential). In this connection, the column $\boldsymbol{\Phi}$ is divided into an active $\boldsymbol{\Phi}^{\mathrm{a}}$ and a sensorial (free) $\boldsymbol{\Phi}^{\mathrm{s}}$ parts, so that system (36) can be written in the form

$$\begin{bmatrix} \mathbf{K}_{uu} & \mathbf{K}_{u\varphi}^{\mathrm{s}} & \mathbf{K}_{u\varphi}^{\mathrm{a}} \\ \mathbf{K}_{\varphi u}^{\mathrm{s}} & \mathbf{K}_{\varphi\varphi}^{\mathrm{ss}} & \mathbf{K}_{\varphi\varphi}^{\mathrm{sa}} \\ \mathbf{K}_{\varphi u}^{\mathrm{a}} & \mathbf{K}_{\varphi\varphi}^{\mathrm{as}} & \mathbf{K}_{\varphi\varphi}^{\mathrm{aa}} \end{bmatrix} \begin{bmatrix} \mathbf{U} \\ \boldsymbol{\Phi}^{\mathrm{s}} \\ \boldsymbol{\Phi}^{\mathrm{a}} \end{bmatrix} = \begin{bmatrix} \mathbf{F}_p + \mathbf{F}_{u\theta} \\ \mathbf{F}_{\varphi\theta}^{\mathrm{s}} \\ \mathbf{F}_q^{\mathrm{a}} + \mathbf{F}_{\varphi\theta}^{\mathrm{a}} \end{bmatrix},$$

$$\mathbf{K}_{\varphi u}^{\mathrm{s}} = (\mathbf{K}_{u\varphi}^{\mathrm{s}})^T, \quad \mathbf{K}_{\varphi u}^{\mathrm{a}} = (\mathbf{K}_{u\varphi}^{\mathrm{a}})^T, \quad \mathbf{K}_{\varphi\varphi}^{\mathrm{as}} = (\mathbf{K}_{\varphi\varphi}^{\mathrm{sa}})^T, \tag{38}$$

where the superscripts s and a indicate the sensorial and active parts of the corresponding matrices. In order not to complicate the numerical analysis [1, 3, 4], it is assumed additionally that $\mathbf{F}_q^{\mathrm{s}} = \mathbf{0}$.

Further, the standard procedure of collecting elements in an ensemble is used. As a result, we obtain a global system of linear algebraic equations describing the thermoelectroelastic state of a layered composite shell:

$$\widetilde{\mathbf{K}}_{uu}\widetilde{\mathbf{U}} + \widetilde{\mathbf{K}}_{u\varphi}^{\mathrm{s}}\widetilde{\boldsymbol{\Phi}}^{\mathrm{s}} = \widetilde{\mathbf{F}}_p + \widetilde{\mathbf{F}}_{u\theta} - \widetilde{\mathbf{K}}_{u\varphi}^{\mathrm{a}}\widetilde{\boldsymbol{\Phi}}^{\mathrm{a}}, \tag{39}$$

$$\widetilde{\mathbf{K}}_{\varphi u}^{\mathrm{s}}\widetilde{\mathbf{U}} + \widetilde{\mathbf{K}}_{\varphi\varphi}^{\mathrm{ss}}\widetilde{\boldsymbol{\Phi}}^{\mathrm{s}} = \widetilde{\mathbf{F}}_{\varphi\theta}^{\mathrm{s}} - \widetilde{\mathbf{K}}_{\varphi\varphi}^{\mathrm{sa}}\widetilde{\boldsymbol{\Phi}}^{\mathrm{a}}, \tag{40}$$

$$\widetilde{\mathbf{F}}_q^{\mathrm{a}} = \widetilde{\mathbf{K}}_{\varphi u}^{\mathrm{a}}\widetilde{\mathbf{U}} + \widetilde{\mathbf{K}}_{\varphi\varphi}^{\mathrm{as}}\widetilde{\boldsymbol{\Phi}}^{\mathrm{s}} + \widetilde{\mathbf{K}}_{\varphi\varphi}^{\mathrm{aa}}\widetilde{\boldsymbol{\Phi}}^{\mathrm{a}} - \widetilde{\mathbf{F}}_{\varphi\theta}^{\mathrm{a}}. \tag{41}$$

From Eq. (40), we have

$$\widetilde{\boldsymbol{\Phi}}^{\mathrm{s}} = (\widetilde{\mathbf{K}}_{\varphi\varphi}^{\mathrm{ss}})^{-1}(\widetilde{\mathbf{F}}_{\varphi\theta}^{\mathrm{s}} - \widetilde{\mathbf{K}}_{\varphi u}^{\mathrm{s}}\widetilde{\mathbf{U}} - \widetilde{\mathbf{K}}_{\varphi\varphi}^{\mathrm{sa}}\widetilde{\boldsymbol{\Phi}}^{\mathrm{a}}). \tag{42}$$

Inserting column (42) into Eq. (39), we arrive at the resolving equation for determining the global displacement vector

$$[\widetilde{\mathbf{K}}_{uu} - \widetilde{\mathbf{K}}_{u\varphi}^{\mathrm{s}}(\widetilde{\mathbf{K}}_{\varphi\varphi}^{\mathrm{ss}})^{-1}\widetilde{\mathbf{K}}_{\varphi u}^{\mathrm{s}}]\widetilde{\mathbf{U}} = \widetilde{\mathbf{F}}_p + \widetilde{\mathbf{F}}_{u\theta} - \widetilde{\mathbf{K}}_{u\varphi}^{\mathrm{s}}(\widetilde{\mathbf{K}}_{\varphi\varphi}^{\mathrm{ss}})^{-1}\widetilde{\mathbf{F}}_{\varphi\theta}^{\mathrm{s}}$$

$$+ [\widetilde{\mathbf{K}}_{u\varphi}^{\mathrm{s}}(\widetilde{\mathbf{K}}_{\varphi\varphi}^{\mathrm{ss}})^{-1}\widetilde{\mathbf{K}}_{\varphi\varphi}^{\mathrm{sa}} - \widetilde{\mathbf{K}}_{u\varphi}^{\mathrm{a}}]\widetilde{\boldsymbol{\Phi}}^{\mathrm{a}}. \tag{43}$$

Based on the numerical algorithm described, a geometrically exact 3-D bilinear finite element EG7P4 was elaborated, which makes it possible to solve the coupled actuator and sensor problems of thermoelectroelasticity for thin-walled structures made of layered composites.

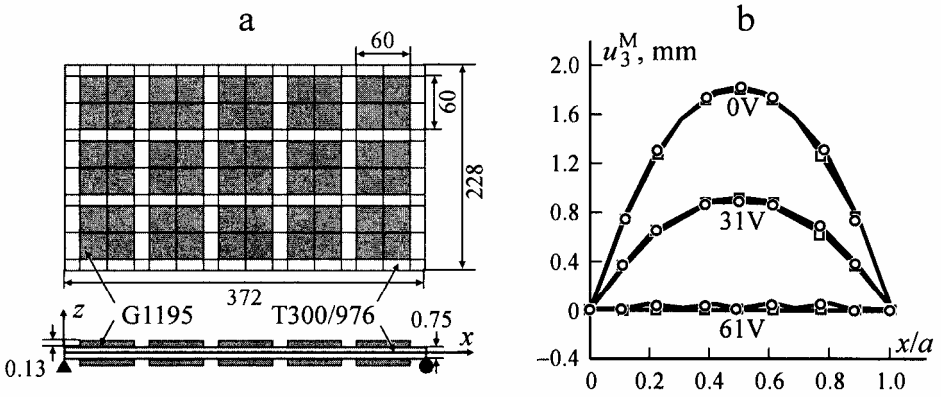

Fig. 3. Scheme of a hinge-supported layered plate with segmented piezoceramic patches: geometry and the finite-element mesh (a) and the distribution of the transverse displacement $u_3^M(x, b/2)$ of midplane along the central line of the plate (b), determined on the basis of the EG7P4 finite element (○) and the 3-D theory of thermopiezoelectricity [16] (□). Dimensions in millimeters.

Numerical Results and Discussion

1. Let us consider a six-layer $[0/45/-45]_s$ plate made of a T300/976 CFRP. The plate is hinge-supported along the edges parallel to the *Oy* axis, while the edges parallel to the *Ox* axis are free. On face surfaces of the plate, 30 square patches made of a G1195 piezoceramic are pasted. The geometrical parameters of the plate are (Fig. 3a) $a = 372$ mm, $b = 228$ mm, $h = 0.75$ mm, and $h_{PZT} = 0.13$ mm [16]; the mechanical constants of CFRP — $E_1 = 150$ GPa, $E_2 = E_3 = 9$ GPa, $\nu_{12} = \nu_{13} = \nu_{23} = 0.3$, $G_{12} = G_{13} = 7.1$ GPa, $G_{23} = 2.5$ GPa, $\alpha_1 = -1.1 \cdot 10^{-6}$ K^{-1}, and $\alpha_2 = \alpha_3 = 2.5 \cdot 10^{-6}$ K^{-1}; the mechanical and piezoelectric constants of piezoceramic — $E_1 = E_2 = E_3 = 63$ GPa, $\nu_{12} = \nu_{13} = \nu_{23} = 0.3$, $G_{12} = G_{13} = G_{23} = 24.2$ GPa, $\alpha_1 = \alpha_2 = \alpha_3 = 9 \cdot 10^{-7}$ K^{-1}, $d_{31} = d_{32} = 0.254$ nm/V, $d_{33} = 0.374$ nm/V, $d_{15} = d_{24} = 0.584$ nm/V, $\epsilon_{11} = \epsilon_{22} = 15.3$ nF/m, and $\epsilon_{33} = 15$ nF/m. The plate is subjected to the following thermal loading: 50°C on the upper surface and –50°C on the lower one at an initial ambient temperature of 20°C. The piezoelectric patches on the internal and external surfaces of the plate are polarized in opposite directions, and the electrodes at interfaces between the patches and the plate are grounded.

The problem was simulated by using a nonuniform mesh of 16 × 10 EG7P4 geometrically exact shell elements. Figure 3b shows the relations between the transverse displacement $u_3^M(x, b/2)$ of the central line of the plate and the longitudinal coordinate x in the absence of electric action and under the action of electric potentials of 31 and 61 B applied to the external surfaces of patches. The results were compared with those obtained on the basis of a three-dimensional isoparametric finite element [16]. As seen, the results obtained agree well with data from the 3-D theory of thermopiezoelectricity. This fact demonstrates that it is important to allow for the transverse compression in problems on calculating thin-walled composite structures subjected to thermoelectromechanical actions.

2. Now, we will examine a sensor problem of electroelasticity for a homogeneous piezoceramic cylindrical shell subjected to a uniformly distributed load of $p_3^+ = 656.17$ N/m on the external surface Ω^+ along two diametrically opposite lines (Fig. 4). The geometrical parameters of the shell correspond to those used in [17]: $R = 291$ mm, $l = 304.8$ mm, and $h = 4$ mm. The mechanical and piezoelectric constants of the PZT-4 piezoceramic are [17] $E_1 = E_2 = 81.3$ GPa, $E_3 = 64.5$ GPa, $\nu_{12} = 0.329$, $\nu_{13} = \nu_{23} = 0.432$, $G_{12} = 30.6$ GPa, $G_{13} = G_{23} = 25.6$ GPa, $e_{31} = e_{32} = -5.2$ C/m^2, $e_{33} = 15.08$ C/m^2, $e_{15} = e_{24} = 12.72$

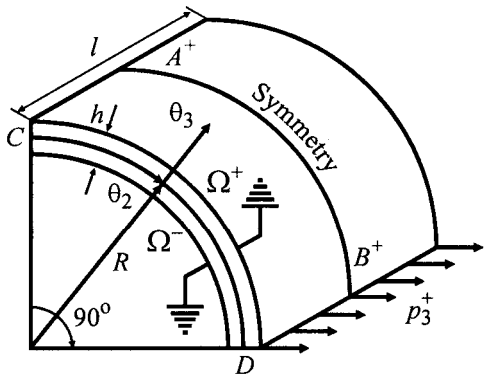

Fig. 4. Calculation scheme of a piezoceramic closed cylindrical shell.

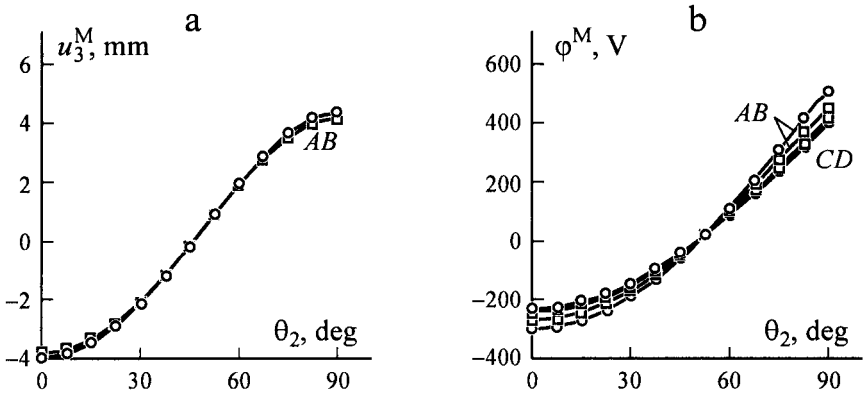

Fig. 5. Distribution of the transverse displacement $u_3^M(l/2, \theta_2)$ of midsurface along the central arc AB (a) and electric potentials on the midsurface $\varphi^M(l/2, \theta_2)$ along the central arc AB (a) and along the arc CD at the free edge (b), determined on the basis of the EG7P4 finite element (○) and a 3-D isoparametric shell element [17] (□) for a piezoceramic closed cylindrical shell.

C/m^2, $\epsilon_{11} = \epsilon_{22}$ = 13.054 nF/m, and ϵ_{33} = 11.505 nF/m. The piezoelectric material is polarized in the transverse direction θ_3, and the electrodes on the internal and external surfaces of the shell are grounded. It is obvious that the calculation of homogeneous shells with the boundary conditions specified on the external surfaces Ω^- and Ω^+, according to approximation (8), leads to a trivial solution for the electric potential, i.e., $\varphi = 0$ everywhere in the shell body. For a correct solution of the problem, the shell was divided across its thickness into four fictitious layers of equal thickness h_n = 1 mm.

Due to symmetry of the problem, an eighth part of the shell was considered, which was simulated by employing uniform meshes of EG7P4 geometrically exact bilinear shell elements. Figure 5 illustrates distributions of the transverse displacement u_3^M and the electric potential φ^M along the arcs AB and CD, belonging to the shell midsurface, obtained by using a 2 × 24

TABLE 1. Transverse Displacement and Electric Potential at a Point A on the Midsurface

Parameter	Mesh							
	1 × 3	1 × 6	1 × 12	1 × 24	2 × 3	2 × 6	2 × 12	2 × 24
u_3^M (A), mm	3.074	3.667	3.831	3.873	3.126	3.734	3.901	3.944
$10^{-2}\varphi^M$ (A) V	2.501	2.650	2.697	2.708	2.737	2.919	2.969	2.981

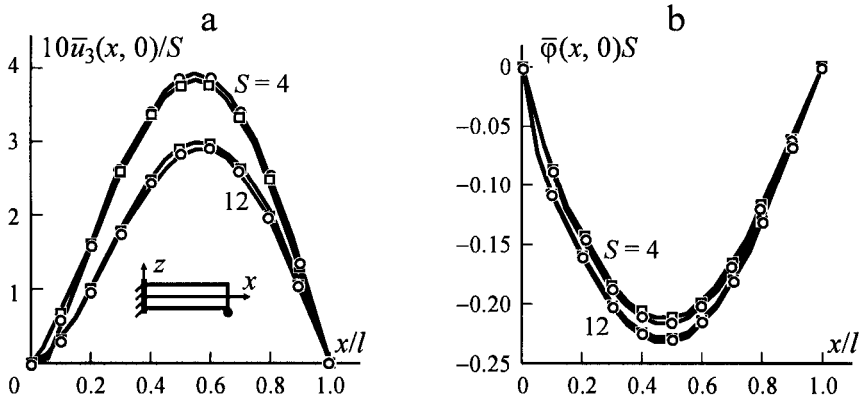

Fig. 6. Distribution of the transverse displacement (a) and electric potential (b) in the longitudinal direction at $N = 8$ determined on the basis of the EG7P4 finite element (○) and the exact solution of the plane problem of thermopiezoelectricity [18] (□) for a piezoceramic plate fixed at the left edge and hinged at the right one.

finite-element mesh. A comparison with results from solving the problem with the help of a 3-D isoparametric quadratic shell element [17] based on the discrete structural approach for the case $N = 4$ is presented. The corresponding calculation data show a good agreement. The additional information on the convergence of the EG7P4 geometrically exact shell element is presented in Table 1. The data of the table point to the possibility of using rather sparse finite-element meshes, which, in turn, allows one to efficiently apply the computer code developed to the controllers of adaptive structures.

3. Let us consider the cylindrical bending of a homogeneous plate of length l and thickness h made of a PZT-5A piezoceramic and rigidly fixed at the left edge ($x = 0$) and hinge-supported or free at its right edge ($x = l$). We choose the following mechanical, piezoelectric, and thermal constants for the material [18]: $C_{11} = C_{22} = 99.201$ GPa, $C_{33} = 86.856$ GPa, $C_{12} = 54.016$ GPa, $C_{13} = C_{23} = 50.778$ GPa, $C_{44} = C_{55} = 21.100$ GPa, $C_{66} = 22.593$ GPa, $e_{31} = e_{32} = -7.209$ C/m^2, $e_{33} = 15.118$ C/m^2, $e_{15} = e_{24} = 12.322$ C/m^2, $\in_{11} = \in_{22} = 15.3$ nF/m, $\in_{33} = 15.0$ nF/m, $\gamma_1 = \gamma_2 = 3.314 \cdot 10^5$ Pa/K, $\gamma_3 = 3.260 \cdot 10^5$ Pa/K, and $g_3 = 7 \cdot 10^{-4}$ C/(K · m^2). On the lower surface $z = -h/2$, a zero temperature is maintained, i.e., $\Theta^- = 0$; on the upper surface $z = h/2$, the temperature distributed by the sinusoidal law $\Theta^+ = \Theta_0 \sin(\pi x/l)$ is kept. It is also assumed that the temperature is distributed linearly across the plate thickness, and the electrodes on both face surfaces are grounded, i.e., $\varphi^- = \varphi^+ = 0$.

Figures 6 and 7 show dependences for the transverse displacement $\bar{u}_3 = u_3/l\alpha_0\Theta_0$ and the electric potential $\bar{\varphi} = e_0\varphi/C_0 l\alpha_0\Theta_0$ for some values of the thin-wallness parameter $S = l/h$ ($C_0 = 99.201$ GPa, $e_0 = 7.209$ C/m^2, and $\alpha_0 = 1.5$

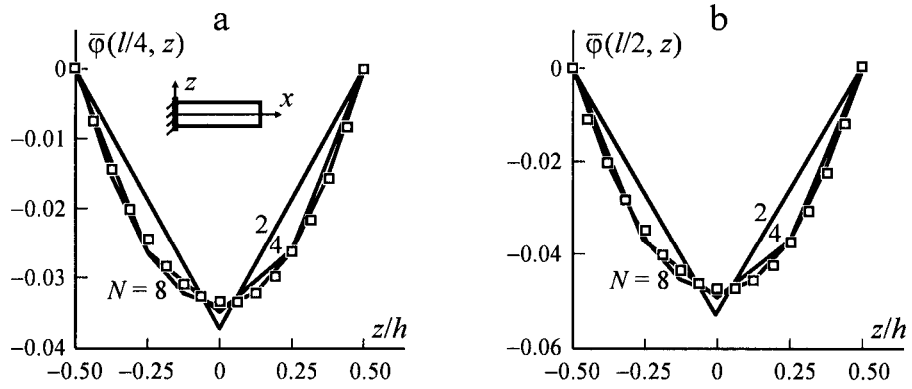

Fig. 7. Distribution of the electric potential $\bar{\varphi}$ in the transverse direction at $x = l/4$ (a) and $x = l/2$ (b), determined on the basis of the EG7P4 finite element (—) and the exact solution of the plane problem of thermopiezoelectricity [18] (□) for a cantilever piezoceramic plate at $S = 4$.

$\cdot 10^{-6}$ K^{-1}). The plate was simulated with the help of 20 finite elements characterizing the plane strain state of the plate; across its thickness, the plate was divided into N layers of equal thickness, so that to describe the spatial character of distribution of the electric potential in the transverse direction more precisely. The cases $N = 2$, 4, and 8 were considered. A comparison with an exact solution of the plane problem of thermoelectroelasticity [18] shows that the division of rather thick plates into four and more layers leads to a calculation accuracy quite acceptable for engineering practice.

In a subsequent study, the present authors are going to generalize the results obtained and apply them to calculating layered piezoelectric shells in the presence of unilateral restrictions [19].

This study was supported by the Ministry of Education and Science of the Russian Federation (Project No. 2.1.1/660).

REFERENCES

1. K. Y. Sze, L. Q. Yao, and S. Yi, "A hybrid stress ANS solid-shell element and its generalization for smart structure modelling. Pt. II. Smart structure modeling," Int. J. Numer. Meth. Eng., **48**, No. 4, 565-582 (2000).
2. S. Lee, N. S. Goo, H. C. Park, K. J. Yoon, and C. Cho, "A nine-node assumed strain shell element for analysis of a coupled electro-mechanical system," Smart Mater. Struct., **12**, No. 3, 355-362 (2003).
3. S. Zheng, X. Wang, and W. Chen, "The formulation of a refined hybrid enhanced assumed strain solid shell element and its application to model smart structures containing distributed piezoelectric sensors/actuators," Smart Mater. Struct., **13**, No. 4, N43-N50 (2004).
4. X. G. Tan and L. Vu-Quoc, "Optimal solid shell element for large-deformable composite structures with piezoelectric layers and active vibration control," Int. J. Numer. Meth. Eng., **64**, No. 15, 1981-2013 (2005).
5. S. Klinkel and W. Wagner, "A geometrically non-linear piezoelectric solid shell element based on a mixed multi-field variational formulation," Int. J. Numer. Meth. Eng., **65**, No. 3, 349-382 (2006).
6. S. Lentzen, "Nonlinearly coupled thermopiezoelectric modelling and FE-simulation of smart structures," Fortschritt-Berichte VDI, **20,** No. 419, VDI Verlag, Dusseldorf (2009).
7. G. M. Kulikov, "Deformation relations exactly representing large rigid-body displacements of shells," Mekh. Tverd. Tela, **39**, No. 5, 130-140 (2004).

8. G. M. Kulikov and S. V. Plotnikova, "Non-linear strain–displacement equations exactly representing large rigid-body motions. Pt. II. Enhanced finite element technique," Comput. Meth. Appl. Mech. Eng., **195**, Nos. 19-22, 2209-2230 (2006).
9. Kulikov G. M. and S. V. Plotnikova, "Calculation of composite structures subjected to follower loads by using a geometrically exact shell element," Mech. Compos. Mater., **45**, No. 6, 545-556 (2009).
10. G. M. Kulikov and E. Carrera, "Finite deformation higher-order shell models and rigid-body motions," Int. J. Solids Struct., **45**, Nos. 11-12, 3153-3172 (2008).
11. D. A. Saravanos, "Mixed laminate theory and finite element for smart piezoelectric composite shell structures," AIAA J., **35**, No. 8, 1327-1333 (1997).
12. G. M. Kulikov and S. V. Plotnikova, "Exact geometry piezoelectric solid-shell element based on the 7-parameter model," Mech. Adv. Mater. Struct., **17** (2010) (in print).
13. W. Novacki, Electromagnetic Effects in Solid Bodies [Russian translation], Mir, Moscow (1986).
14. G. M. Kulikov and S. V. Plotnikova, "Geometrically exact four-node piezoelectric solid-shell element," Mech. Adv. Mater. Struct., **15**, Nos. 3-4, 199-207 (2008).
15. G. M. Kulikov and S. V. Plotnikova, "Finite rotation geometrically exact four-node solid-shell element with seven displacement degrees of freedom," Comput. Model. Eng. Sci., **28**, No. 1, 15-38 (2008).
16. S. K. Ha, C. Keilers, and F.-K. Chang, "Finite element analysis of composite structures containing distributed piezoceramic sensors and actuators," AIAA J., **30**, No. 3, 772-780 (1992).
17. P. Heyliger, K. C. Pei, and D. Saravanos, "Layerwise mechanics and finite element model for laminated piezoelectric shells," AIAA J., **34**, No. 11, 2353-2360 (1996).
18. S. S. Vel and R. C. Batra, "Generalized plane strain thermopiezoelectric analysis of multilayered plates," J. Therm. Stresses, **26**, No. 4, 353-377 (2003).
19. G. M. Kulikov and S. V. Plotnikova, "Contact interaction of composite shells, subjected to follower loads, with a rigid convex foundation," Mech. Compos. Mater., **46**, No. 43-56 (2010).